CERN–PPE/94–167
28 October 1994

A New Tuning Method for Ionization Energy Loss Calculations

Olof Bärring

PPE/DEE Division

Abstract

In order to improve the accordance between measured and calculated energy loss distributions a new tuning method is suggested. The idea is that the oscillator strength function or, equivalently, the dielectric function of the specific medium used in the detector can be extracted from a deconvoluted well measured dE/dx spectrum. This procedure involves rather delicate numerical problems, which will be discussed in detail. The method is in particular suitable for detectors with thin layered sampling ($xP < 1$ cm) where traditional methods tend to fail due to the difficulties of correcting for detector inefficiencies and smearing. This is illustrated by testing the method on data from a thin layered *Time Projection Chamber*, TPC.

(Submitted to Nuclear Instruments and Methods A)

1 Introduction

The measurement of the ionization energy loss (dE/dx) of a charged particle in a gas filled proportional chamber is still one of the most important means for particle identification in the Lorentz factor range $\gamma \sim 4 - 300$. Due to competing requirements of minimal loss of particles inside the detector, fast response and also good tracking capabilities todays *Time Projection Chambers* (TPCs) have a comparable low value on the product of sampling length and pressure (xP), usually in the region 0.5–1 cm$\times$atm. From the point of view of dE/dx this has the advantage of giving a high Fermi plateau but the resolution becomes worse unless the number of samplings per track is increased. Another problem which arises is that various smearing effects of the measured amplitudes become sizable compared to the intrinsic energy loss. The simulation of the dE/dx therefore becomes more complicated. Further calibrations are usually also necessary since the detector conditions may change with time for various reasons; e.g. the pressure, gas mixture and temperature can vary with the surrounding conditions, variations in beam luminosity or background may increase the space charge etc.. All such effects must be taken into account in the simulation of the ionization energy loss. For those reasons but also because the solution of the problem is interesting in itself we present in this paper a method to tune globally the dE/dx simulations to the detector response.

The basic assumption, which validates the method proposed here, is that all properties of the detector itself can be contained in one single function which is independent of the kinematics of the incident charged particle. This is clearly the case for the intrinsic energy loss where the dielectric function, or equivalently the oscillator density function, contains all the electro-magnetic properties of the medium. It does not seem to be too unrealistic to further assume that all smearing effects, due to the detector (including the electronic chain) of the intrinsic energy loss, also are independent of the kinematics of the incident particle. Hence it should be possible to define a detector specific dielectric function containing, in addition to the dielectric properties of the medium, also all smearing of the amplitude due to the detector. Since this function uniquely determines the ionization energy loss (Landau-) distribution for any particle and momentum the opposite must also be true, i.e. given a well measured Landau spectrum for a particle of known momentum and type we should be able to calculate the detector specific dielectric function. This procedure involves two specific problems: (1) a deconvolution of the Landau distribution to obtain the single collision cross section and (2) determination of the dielectric function from the single collision cross section. The first problem may be solved by an appropriate parametrization of the measured Landau spectrum as will be shown in next section. The dielectric function is related to the single collision cross section via a first order differential equation whose solution will be treated in section 3. In the following section a convenient method to fit the parameterization to data is proposed. Then follows a short discussion on possible numerical problems. Finally, the results are presented where a special effort has been made to show how the different steps in the calculations are performed. The method is applied to data from the TPC detector in the DELPHI experiment at the *Large Electron Positron* (LEP) collider, CERN.

2 De-convolution of the Landau distribution

From the Landau [1] formula for the ionization energy loss,

$$\phi(x,\Delta) = \frac{1}{2\pi i}\int_{\sigma-i\infty}^{\sigma+i\infty} e^{s\Delta}\exp\left\{-xn_e\int_0^\infty \left(1-e^{-sE}\right)\frac{d\sigma}{dE}(E)\,dE\right\}\,ds \tag{1}$$

we may deduce the single collision cross section, $\frac{d\sigma}{dE}$. x is the detector thickness, Δ the energy loss and n_e the number of electrons per unit volume. In the following we will suppress the

explicit dependence on x in ϕ ($\phi(x,\Delta) \equiv \phi(\Delta)$) and its Laplace transform ($\hat{\phi}(x,\Delta) \equiv \hat{\phi}(\Delta)$).

By Laplace transforming (1) and taking the derivative with respect to s on both sides, we get

$$\hat{\phi}(s) \equiv \int_0^\infty e^{-s\Delta}\phi(\Delta)\,d\Delta = \exp\left\{-xn_e\int_0^\infty \left(1-e^{-sE}\right)\frac{d\sigma}{dE}(E)\,dE\right\} \tag{2}$$

and

$$\hat{\phi}'(s) = \int_0^\infty e^{-s\Delta}(-\Delta)\phi(\Delta)\,d\Delta = xn_e\int_0^\infty e^{-sE}(-E)\frac{d\sigma}{dE}(E)\,dE \exp\left\{-xn_e\int_0^\infty \left(1-e^{-sE}\right)\frac{d\sigma}{dE}(E)\,dE\right\} \tag{3}$$

Dividing equation (3) and (2) gives:

$$\frac{\hat{\phi}'(s)}{\hat{\phi}(s)} = xn_e\int_0^\infty e^{-sE}(-E)\frac{d\sigma}{dE}(E)\,dE \tag{4}$$

The integral on the right hand side is the Laplace transform of $(-E)\,\frac{d\sigma}{dE}(E)$, which we may use to finally get:

$$\frac{d\sigma}{dE}(E) = -\frac{1}{xn_eE}\frac{1}{2\pi i}\int_C e^{sE}\frac{\hat{\phi}'(s)}{\hat{\phi}(s)}\,ds \tag{5}$$

Given that $\hat{\phi}$ is analytic with no other types of singularities than poles in the domain T, holomorphe and nonzero on the contour C of that domain the integral in (5) can be evaluated:

$$\frac{1}{2\pi i}\int_C e^{sE}\frac{\hat{\phi}'(s)}{\hat{\phi}(s)}\,ds = \sum_k \zeta_k e^{z_kE} - \sum_k \xi_k e^{p_kE} \tag{6}$$

where $z_k \in T$ are the zeros of order ζ_k and $p_k \in T$ are the poles of order ξ_k to $\hat{\phi}(s)$. The proof of (6) can be found in any standard text on the theory of complex integrals, see for instance [2].

The result (5) together with (6) is remarquable; the single collision cross section $\frac{d\sigma}{dE}$ is completely determined by the zeros and poles of the Laplace transformed Landau distribution. The integral in the exponent in (1) exists in the lower limit if

$$\exists A>0, \delta>0, \alpha>0 : \left|\frac{d\sigma}{dE}(E)\right| \leq AE^{\alpha-2},\ \forall E : 0<E\leq\delta \tag{7}$$

(note that $1-e^{-sE} \sim sE$ as $E \to 0$) and in the higher limit if

$$\exists A>0, B>0, \alpha>0 : \left|\frac{d\sigma}{dE}(E)\right| \leq AE^{-\alpha-1},\ \forall E : B\leq E<\infty \tag{8}$$

The former condition is always fulfilled by (5) whereas the latter imposes $\Re(z_k) < 0$ and $\Re(p_k) < 0$, i.e. the contour "C" in (6) should only enclose the roots and zeros in the left half plane.

Now, as will be seen in section 5, it is usually possible to fit the following function to the measured $\phi(\Delta)$

$$\phi(\Delta) \approx g(\Delta) = \sum_{j=1}^{n}\alpha_j\Delta^j e^{-\beta_j\Delta} \tag{9}$$

which is a particularly useful parametrization since its Laplace transform is purely rational,

$$\hat{g}(s) = \sum_{i=1}^{n} \alpha_i \frac{i!}{(s+\beta_i)^{i+1}} \tag{10}$$

From (10) we can immediately read out the poles: $p_i = -\beta_i$ with $\xi_i = i+1$.

The remaining problem is to determine the zeros (γ_j) of $\hat{g}(s)$. Multiplying (10) with $(s+\beta_1)^2(s+\beta_2)^3 \cdot \ldots \cdot (s+\beta_n)^{n+1}$ we get a polynom of degree $\leq (n+2)(n+1)/2 - 3$. The polynomial equation thus obtained can be solved numerically if n is reasonably small (e.g. $n = 4$ results in a 12th degree polynomial) and the roots (γ_i) are in general complex.

To summarize, with (10), (6) and (5) our approximate single collision cross section becomes

$$\frac{d\sigma}{dE}(E) \approx \frac{1}{x n_e E} \left(\sum_{i=1}^{n} (i+1) e^{-\beta_i E} - \sum_{j=1}^{N} e^{\gamma_j E} \right) \tag{11}$$

$$N \leq \frac{(n+2)(n+1)}{2} - 3$$

where we note that $x n_e E \, \frac{d\sigma}{dE}(E) \to A \geq 2$ as $E \to 0$.

3 The Dielectric Function

The electro dynamic properties of the detector medium are completely contained in the complex dielectric function, $\epsilon(E) = \epsilon_1(E) + i\epsilon_2(E)$, where ϵ_1 and ϵ_2 are real. An alternative quantity is the *Oscillator Strength Density*, which we denote $f(E)$ in the following. The functions $f(E)$ and $\epsilon_2(E)$ are approximately related through:

$$\epsilon_2(E) \approx \frac{\pi}{2} (\hbar v_p)^2 \frac{f(E)}{E} \tag{12}$$

where v_p is the plasma frequency of the detector medium ($\hbar v_p \approx 0.82$ eV for argon at NTP). The imaginary part of the dielectric function uniquely determines the real part, ϵ_1, via the Kramer-Kronig relation:

$$\epsilon_1(E) = 1 + \frac{2}{\pi} \int_0^\infty \frac{\xi \epsilon_2(\xi)}{\xi^2 - E^2} \, d\xi \tag{13}$$

where the Cauchy principal value of the integral should be taken.

We aim to determine $\epsilon(E)$ (or $f(E)$) from the single collision cross section $\frac{d\sigma}{dE}(E)$ which we in turn extracted from the Landau distribution as described in previous section. To this end we need an expression which relates ϵ and $\frac{d\sigma}{dE}$. An useful approximate equation is for instance given in appendix C in a paper of Lapique and Piuz [3],

$$n_e \frac{d\sigma}{dE}(E) = \frac{A}{\beta^2} \left\{ \frac{f(E)}{E} \left[\log\left(\frac{2 m_e c^2 \beta^2}{(1-\beta^2)E} \right) - \beta^2 \right] + \frac{1}{E^2} \int_0^E f(\xi) \, d\xi - \Theta(E,\beta) \right\} \tag{14}$$

where $A = 0.1536 z^2 (Z/A_0) \rho$ MeV/cm, ze, β, Z, A_0 and ρ are the charge and velocity of the incident particle, atomic number, mass number and density of the medium respectively. m_e is the electron rest mass and Θ is the density correction,

$$-\Theta(E,\beta) = \frac{f(E)}{E} \left[\log\left(\frac{1-\beta^2}{|1-\beta^2\epsilon|} \right) + \beta^2 (1 - \epsilon_1) \right] + \frac{2}{(\hbar v_p)^2} \left(\beta^2 - \frac{\epsilon_1}{|\epsilon|^2} \right) \tag{15}$$

which is small for $\gamma \lesssim 20 - 30$ ($\gamma^2 = 1/(1-\beta^2)$).

It is instructive to study the equation without the density term. Then (14) becomes a first order differential equation for which we easily find an analytic solution. Let $F(E) = \int_0^E f(x)dx$:

$$-F'(E)(\beta^2 + \log(E/E_{max}) + \frac{F(E)}{E} = H(E) \tag{16}$$

which can be written as

$$\frac{d}{dE}\left(\frac{F(E)}{\beta^2 + \log(E/E_{max})}\right) = -\frac{H(E)}{(\beta^2 + \log(E/E_{max}))^2} \tag{17}$$

where

$$E_{max} = \frac{2m_e c^2 \beta^2}{1-\beta^2} \tag{18}$$

$$H(E) = \frac{\beta^2 n_e E}{A}\frac{d\sigma}{dE}(E) \tag{19}$$

Integrating (17) gives,

$$F(E) = -(\beta^2 + \log(E/E_{max}))\left(C_1 + \int_0^E \frac{H(\xi)}{(\beta^2 + \log(\xi/E_{max}))^2}\, d\xi\right) \tag{20}$$

where C_1 is an integration constant. There are two singularities which should be investigated: $E \to 0$ and $\beta^2 + \log(E/E_{max}) \to 0$. In the limit $E \to 0$ we have:

$$\begin{aligned} 0 \le \lim_{x\to 0}\left|\log(x)\int_0^x \frac{d\xi}{\log^2(\xi)}\right| &= \lim_{x\to 0}\left|\log(x)\int_{-\infty}^{log(x)}\frac{e^t\,dt}{t^2}\right| \\ \le \lim_{x\to 0}\left|\frac{1}{\log(x)}\int_{-\infty}^{log(x)} e^t\,dt\right| &= \lim_{x\to 0}\left|\frac{x}{\log(x)}\right| = 0 \end{aligned} \tag{21}$$

and since H behaves well in origo:

$$\begin{aligned} \lim_{E\to 0} -(\beta^2 + \log(E/E_{max}))\left(C_1 + \int_0^E \frac{H(\xi)}{(\beta^2 + \log(\xi/E_{max}))^2}\, d\xi\right) \\ = \lim_{E\to 0} -(\beta^2 + \log(E/E_{max}))C_1 \end{aligned} \tag{22}$$

from which we conclude that the integration constant C_1 must be zero if we require $F(E)$ to be non-singular in $E = 0$.

In the high energy limit we have:

$$\begin{aligned} \lim_{E\to E_{max}e^{-\beta^2}} &-(\beta^2 + \log(E/E_{max}))\int_0^E \frac{H(\xi)\,d\xi}{(\beta^2 + \log(\xi/E_{max}))^2} \\ &= \lim_{x\to 1} E_{max}e^{-\beta^2}\log(x)\left(\int_0^a \frac{H(\xi E_{max}e^{-\beta^2})\,d\xi}{log^2(\xi)} + \right. \\ &\left. \int_a^x \frac{H(\xi E_{max}e^{-\beta^2})\,d\xi}{log^2(\xi)}\right) \end{aligned}$$

where a is an arbitrary constant chosen as $0 \ll a < x$. The integral from 0 to a is finite; $1/log^2(x) = 0$ in $x = 0$ though all derivatives are infinite. We may expand the logarithm in the second integral and thus single out the singularity. After some algebra one finds:

$$\frac{1}{\log^2(\xi)} = \frac{\xi}{(1-\xi)^2} + \frac{1}{12} - \frac{1}{240}(1-\xi)^2 + \ldots$$

Only the first term on the right hand side contributes to the limit as all others are finite and hence killed by $log(x)$ as $x \to 1$.

$$\lim_{x\to 1} \log(x) \int_a^x \frac{\xi\, d\xi}{(1-\xi)^2} = \lim_{x\to 1} \log(x)(\frac{x}{1-x} + \log(1-x)) = -1$$

Note that this limit is independent of a.

Knowing that $H(E)$ is finite and continuous in $[a, x]$ one can write

$$E_{max}e^{-\beta^2} \inf_{\xi\in[a,1]}(H(\xi E_{max}e^{-\beta^2})) \leq$$
$$-\lim_{x\to 1} E_{max}e^{-\beta^2} \log(x) \int_0^x \frac{H(\xi)\, d\xi}{log^2(\xi)} \leq$$
$$E_{max}e^{-\beta^2} \sup_{\xi\in[a,1]}(H(\xi E_{max}e^{-\beta^2}))$$

where we may let a come arbitrary close to one. Thus:

$$\lim_{E\to E_{max}e^{-\beta^2}} -(\beta^2 + \log(E/E_{max})) \int_0^E \frac{H(\xi)}{(\beta^2 + \log(\xi/E_{max}))^2}\, d\xi = E_{max}e^{-\beta^2} H(E_{max}e^{-\beta^2}) \tag{23}$$

which is exactly what one would expect from the differential equation (16) substituting $E = E_{max}e^{-\beta^2}$.

Since $f(E)$ is a density function it should be positive and hence $F(E)$ should be an monotonous increasing function. This puts some extra requirements on the asymptotic behaviour of the function $H(E)$ which in our case is just a finite sum of exponentials. It can be shown that $F(E)$ gets the mentioned properties if $H(E)$ fulfills:

$$H(E) \geq Ce^{-aE} \qquad \text{for } a \leq \frac{1}{E_{max}e^{-\beta^2}} \tag{24}$$

which in our approximation (11) implies a pole very close to the real axis. From (9) one concludes that such a pole governs the high energy behaviour of the Landau distribution, i.e. far out on the tail, where the information from data is very poor. Therefore we cannot expect $\frac{d\sigma}{dE}(E) \sim H(E)/E$ to have the correct asymptotic behaviour; at some point the approximation breaks down and the obtained oscillator density function $f(E)$ may become negative. This will indeed be seen in the result section below but, as also shown in the same section, the non-physical high energy behaviour of $f(E)$ has no influence on the calculated Landau distributions.

With (20) in (12) (and using $f(E) = F'(E)$) we get a reasonable first approximation for ϵ_2

$$\epsilon_2(E) \approx -\frac{\pi}{2E^2}(\hbar v_p)^2 \int_0^E \frac{H(\xi) + \xi H'(\xi)}{\beta^2 + \log(\xi/E_{max})}\, d\xi \tag{25}$$

($H'(\xi) \equiv dH(\xi)/d\xi$).

The $\epsilon(E) = \epsilon_1(E) + i\epsilon_2(E)$ given by (25) and (13) can be used as a start function for an iterative numerical solution to (14, 15) Ignoring the *Cherenkov* term, $\frac{2}{(\hbar v_p)^2}(\beta^2 - \frac{\epsilon_1}{|\epsilon|^2})$, the iterative equation becomes

$$\epsilon_2(E)_{n+1} = \frac{\frac{\pi\beta^2 n_e(\hbar v)^2}{2A}\frac{d\sigma}{dE}(E) - \frac{1}{E^2}\int_0^E \xi\epsilon_2(\xi)_n\, d\xi}{\log\left(\frac{2m_e c^2\beta^2}{|1-\beta^2\epsilon(E)_n|E}\right) - \beta^2\epsilon_1(E)_n} \tag{26}$$

where we have used (12) to eliminate all $f(E)/E$. $\epsilon(E)_n$ etc. denotes the calculated ϵ after n iterations with $\epsilon(E)_1$ given by (25) and (13). One usually reaches reasonable convergens after only a few iterations.

Two constants enter in the formulae above: E_{max}, the maximum energy transfer in a single collision, and v_p, the plasma frequency of the detector medium. Those constants should in principle be scaled from eV to the same energy unit as is measured by the detector, e.g. the ionization corresponding to one flash ADC count. However, as they are material constants of the detector medium they can both be used for further fine tuninig the kinematic dependence in (14) and (15) if, for instance, a second Landau spectrum or the truncated mean ($\langle dE/dx \rangle$) vs. $\beta\gamma$ has been measured.

4 The Fit Procedure

The fit of the function $g(\Delta)$ (9) to the measured Landau distribution is a standard numerical problem. The iterative scheme to find a solution to the system of minimization equations proposed in this section is reasonable stable and easy to implement. The integrals are carried out analytically as far as possible in order to reduce the numerical work and uncertainties.

We want to minimize

$$I(\boldsymbol{\alpha},\boldsymbol{\beta}) = \int_0^\infty \left(\phi(x) - \sum_{j=1}^{n} \alpha_j x^j e^{-\beta_j x} \right)^2 dx \tag{27}$$

where $\phi(x)$ is the measured Landau distribution and

$$\boldsymbol{\alpha} = (\alpha_1, \alpha_2, \ldots, \alpha_n) \tag{28}$$

$$\boldsymbol{\beta} = (\beta_1, \beta_2, \ldots, \beta_n) \tag{29}$$

The minimum is determined by setting the gradient to zero: $\nabla_{\boldsymbol{\alpha},\boldsymbol{\beta}} I(\boldsymbol{\alpha},\boldsymbol{\beta}) = \mathbf{0}$, which corresponds to a system of $2n$ equations,

$$0 = \frac{\partial I}{\partial \alpha_i} = -2 \int_0^\infty x^i e^{-\beta_i x} \left(\phi(x) - \sum_{j=1}^{n} \alpha_j x^j e^{-\beta_j x} \right) dx \tag{30}$$

$$0 = \frac{\partial I}{\partial \beta_i} = 2 \int_0^\infty \alpha_i x^{i+1} e^{-\beta_i x} \left(\phi(x) - \sum_{j=1}^{n} \alpha_j x^j e^{-\beta_j x} \right) dx \tag{31}$$

$$(i \in [1, n]\,)$$

After some algebra and rearrangement of the terms we get,

$$\alpha_i \frac{(2i)!}{(2\beta_i)^{2i+1}} = \int_0^\infty x^i e^{-\beta_i x} \phi(x)\, dx \; - \sum_{j \neq i} \alpha_j \frac{(i+j)!}{(\beta_i + \beta_j)^{i+j+1}} \tag{32}$$

$$\alpha_i \frac{(2i+1)!}{(2\beta_i)^{2i+2}} = \int_0^\infty x^{i+1} e^{-\beta_i x} \phi(x)\, dx \; - \sum_{j \neq i} \alpha_j \frac{(i+j+1)!}{(\beta_i + \beta_j)^{i+j+2}} \tag{33}$$

or

$$
(34)\qquad \begin{cases} \alpha_i &= \dfrac{\int_0^\infty x^i e^{-\beta_i x}\phi(x)\,dx - \sum_{j\neq i}\alpha_j \dfrac{(i+j)!}{(\beta_i+\beta_j)^{i+j+1}}}{\dfrac{(2i)!}{(2\beta_i)^{2i+1}}} \\ \beta_i &= \dfrac{2i+1}{2}\dfrac{\int_0^\infty x^i e^{-\beta_i x}\phi(x)\,dx - \sum_{j\neq i}\alpha_j \dfrac{(i+j)!}{(\beta_i+\beta_j)^{i+j+1}}}{\int_0^\infty x^{i+1} e^{-\beta_i x}\phi(x)\,dx - \sum_{j\neq i}\alpha_j \dfrac{(i+j+1)!}{(\beta_i+\beta_j)^{i+j+2}}} \end{cases}
$$

A further constraint is the normalization, which must be same for the measured and the fitted function:

$$
(35)\qquad \sum_1^n \alpha_i \frac{i!}{\beta^{i+1}} = \int_0^\infty \phi(x)\,dx \;(=1)
$$

Obviously, to get the correct high energy behaviour of $\frac{d\sigma}{dE}$, i.e. $\frac{d\sigma}{dE}(E)\to 0$ as, $E\to\infty$, it must be made sure that all β_i are positive. We may also require that $\alpha_i > 0$ to aviod $\phi(E) < 0$ for some energy outside the interval where the fit was performed. It is therefore necessary to take the absolute value of the right hand sides in (34).

If the energy is scaled so that the measured Landau distribution has its peak around $x = 1$, a good starting point for the iteration is $\alpha_i = 0$ and $\beta_i = (2i+1)/2$.

5 Numerical Considerations

The formulae in section 2–4 have been implemented in a FORTRAN program. It has been found that the proposed iterative solutions (26) and (34) are numerically quite stable and it is usually sufficient with single precision calculations. The by far most difficult step turns out to be the finding of the zeros γ_i of $\hat{g}(s)$ especially when $n > 3$. For this we have used a CERN program library routine ([4]), which calculates the zeros in complex double precision. Because $\frac{d\sigma}{dE}(E)\to 0$ for $E\to\infty$, the roots are required to lie in the left halfplane ($\Re(\gamma_i) < 0$). Therefore, the contour C in (5) and (6) must be chosen to enclose all zeros and poles in $\Re(s) < 0$. Note that whereas the poles are already constrained to fulfil this requirement as was discussed in the end of previous section, the zeros (γ_i) are more difficult to control. In numerical calculations one may thus try to either discard any root with $\Re(\gamma_i) > 0$ or reduce n. This latter choice also protects against unavoidable rounding errors which could be the origin of the "unphysical" roots. Hence the procedure to obtain the results in the following section has been to start with $n = 5$ (18 zeros) and decrease n until the real parts of all the roots are < 0.

6 Results

As an instructive example, and also a demonstration of its functionality and capability, the described tuning method is applied to a given data sample from the *Time Projection Chamber* (TPC) in the DELPHI experiment at the *Large Electron Positron* (LEP) collider, CERN. The characteristics of the TPC are listed in table (1). The data consist of identified (by other means than dE/dx) electrons, muons and pions in $\mathrm{Z}^0 \to \tau^+\tau^-$ decays. Such events serve as a good testing ground for dE/dx since the τ decay products have reasonably large momentum spectra (2–45 GeV/c in the present sample) and they are usually well isolated; more than 86% of the τ decays are 1-prong, i.e. contain only one charged track. Thus, possible effects from electronic undershoot, overlapping ionization clusters etc. will not disturb the measurements. Of course,

active length	2×134 cm
radius	32.5 – 116 cm
volume	$\sim 14\ m^3$
gas	80% argon +20% CH_4
electric field	150 V/cm
magnetic field	1.2 Tesla
pressure	1 atm
wire spacing	0.4 cm
number of wires	192

Table 1: Some characteristics of the DELPHI TPC. Notice the small sampling length, $xP \geq 0.4$ cm atm.

(α_j, β_j)	n=2	n=3	n=4	n=5
(α_1, β_1)	(0.815, 1.397)	(0.464, 1.213)	(0.382, 1.205)	(0.337, 1.181)
(α_2, β_2)	(5.750, 2.703)	(2.663, 2.504)	(1.653, 2.284)	(1.282, 2.221)
(α_3, β_3)		(16.73, 4.130)	(6.126, 3.458)	(4.197, 3.322)
(α_4, β_4)			(81.61, 6.270)	(16.38, 4.650)
(α_5, β_5)				(586.8, 8.950)

Table 2: The parameters of the fits in figure (1).

in the end such effects must also be understood but the clean environment in τ decays is perfect for the first tuning of the dE/dx calculations.

Figure 1 shows a measured Landau spectrum for muons with $p \in [30, 35]$ GeV. In the same figure is shown the fitted functions $g(\Delta)$ for $n = (2, 3, 4, 5)$. Table (2) lists the parameters α_i and β_i for the different fits. In the following it will be shown in detail how the single collision cross section is calculated from the $n = 2$ parametrization of the Landau distribution.

From table (2) we get:

$$g(\Delta) = 0.815\Delta e^{-1.397\Delta} + 5.750\Delta^2 e^{-2.703\Delta}$$

and

$$\hat{g}(s) = \frac{1 \cdot 0.815}{(s + 1.397)^2} + \frac{2 \cdot 5.750}{(s + 2.703)^3}$$

The poles of $\hat{g}$ are $p_1 = -\beta_1 = -1.397$ and $p_2 = -\beta_2 = -2.703$ and the zeros are given by the roots to the polynomial equation

$$0.815(s + 2.703)^3 + 11.5(s + 1.397)^2 = 0 \Longleftrightarrow$$
$$0.815s^3 + 18.11s^2 + 50.0s + 38.54 = 0$$

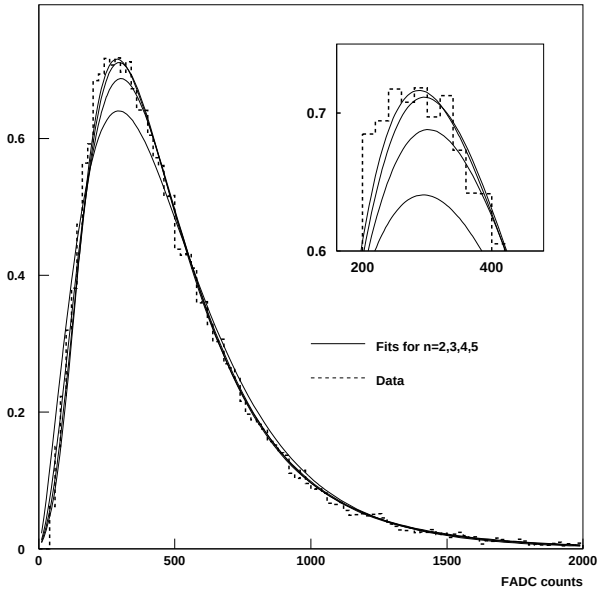

Figure 1: The different fits to the measured Landau distribution. The solid curves shows the fit for n=2,3,4 and 5 corresponding to increasing quality of the fit. The difference between the n=4 and n=5 fits is negligible which can be seen in the magnification of the peak.Here the ionization is measured in the *Flash Analog to Digital Converter* (FADC) counts of the detector electronics.

which is solved numerically. The approximate roots are:

$$\begin{aligned} z_1 &= -19.15 \\ z_2 &= -1.538 + 0.325i \\ z_3 &= -1.538 - 0.325i \end{aligned}$$

All zeros are of single order ($\zeta_1 = \zeta_2 = \zeta_3 = 1$) and the poles are of order 2 and 3 respectively ($\xi_1 = 2$, $\xi_2 = 3$). We may now use the formulae (5, 6) to obtain the approximate $\frac{d\sigma}{dE}$ shown in figure (2),

$$\frac{d\sigma}{dE}(E) = \frac{1}{xn_eE}\left(2e^{-1.397E} + 3e^{-2.703E} - e^{-19.15E} - 2e^{-1.538E}\cos(0.325E)\right) \tag{36}$$

Whereas the poles, β_i, are directly related to the fitted Landau distribution, there is no clear interpretation of the zeros, γ_i. Due to their imaginary parts the zeros may give rise to structures in $\frac{d\sigma}{dE}$, which resemble the edges at threshold energies of the atomic shells apparent when the same function is calculated from, for instance, a tabulation of the photo absorption cross section. However, it is hard to believe that the measured Landau distribution contains such detailed information from the atomic level. It is more likely to be a coincidence.

The calculation of the dielectric function $\epsilon(E) = \epsilon_1(E) + i\epsilon_2(E)$ can now proceed according to the iterative scheme proposed in section 3. Figure (3) depicts the obtained ϵ_2 and also reveals a disturbing behaviour at high E: ϵ_2 becomes negative at $E \gtrsim 1500$. This non-

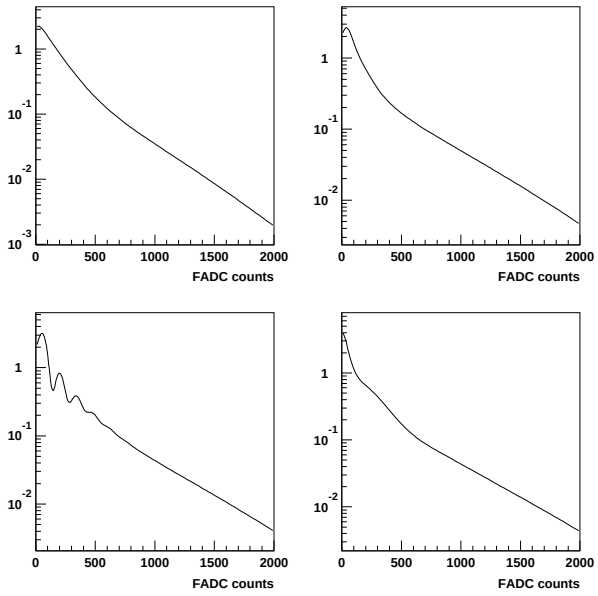

Figure 2: The obtained $E\,\frac{d\sigma}{dE}(E)$ for $n = 2,3,4,5$. For $n = 5$ two roots with $\Re(\gamma_i) > 0$ were discarded according to the discussion in previous section. The y scale in the plots was arbitrarily chosen so that $xn_e = 1$. The structures visible in the $n = 4$ approximation of $E\,\frac{d\sigma}{dE}(E)$ are due to the imaginary parts of the zeros (γ_i) to equation (10).

physical high energy behaviour is probably due to a too fast drop in the tail of the parameterized Landau function, which was already discussed in the end of section 3.

With the obtained $\epsilon_2(E)$ all necessary information needed for calculating any Landau distribution is present. A program, described in [6], calculates the Landau distributions from the oscillator density by means of to (14) and (1). The output is compared with data in figures (4) and (5). Unfortunately no measured Landau distribution of identified (by other means than dE/dx) minimum ionizing pions was available. The two parameters v_p and E_{max} have been fine tuned to fit the truncated mean ($\langle dE/dx \rangle$) vs. $\beta\gamma$ plot shown figure (5).

There is a deviation between the measured $\langle dE/dx \rangle$ for electrons from photon conversion and the calculated curve in figure (5). In the formulae (14) and (15) it is assumed that the incident particle is much heavier than the atomic electrons. This is obviously not a valid approximation when the incident particle is an electron. Further corrections are thus needed but this discussion falls outside the scope of the present paper.

In figure (4) one sees a discrepancy at low energies between measured and calculated spectra. Indeed there is a constant offset in the data whereas the calculated distributions begin in zero. A better low energy behaviour could be achieved if higher terms were included in the fit (equation (9)) but this would lead to practically insolvable polynomial equations for finding the zeros of $\hat{g}(s)$. The simpler way to overcome the problem is to shift the energy scale by the constant offset before doing the fit to the measured Landau distribution. The same shift must then appear throughout the calculations. The predicted Landau distributions when taking into account a constant offset of 50 energy units are shown together with data in figure (6). For mere comparison a biased distribution of minimum ionizing pions was included in the figure.

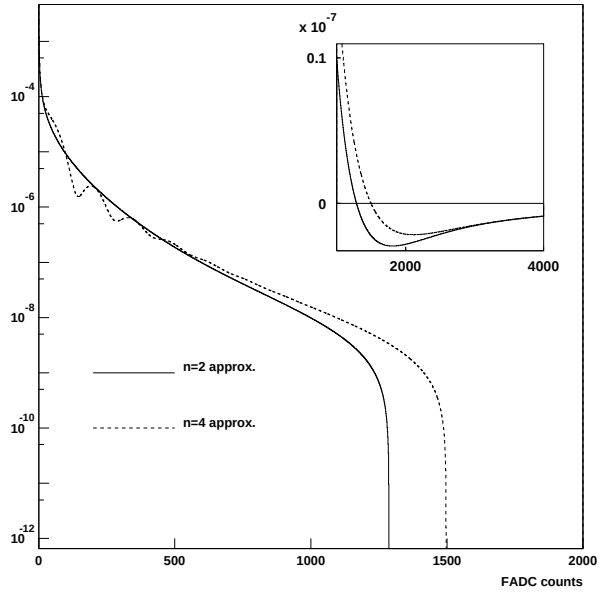

Figure 3: $\epsilon_2(E)$ calculated from the $\frac{d\sigma}{dE}(E)$ in figure (2) with the procedure outlined in section 3. The non-physical high energy behaviour is discussed in the text and in the end of section 3. The solid and dashed lines are the $n = 2$ and $n = 4$ approximations respectively. The in folded picture shows, in linear scale, the region where the approximation breaks down, i.e. ϵ_2 becomes negative.

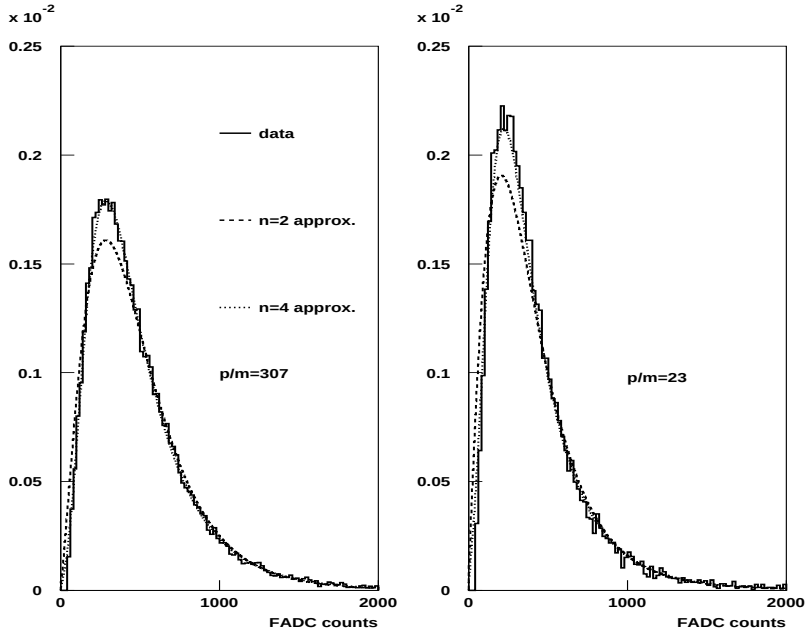

Figure 4: Calculated Landau distributions vs. real data. Note that the measured distribution for 32.5 GeV/c ($p/m \approx 307$) $\mu^{\pm}$ was used in the tuning. The solid line shows the data, dashed and dotted lines are the result from the $n = 2$ and $n = 4$ approximations respectively.

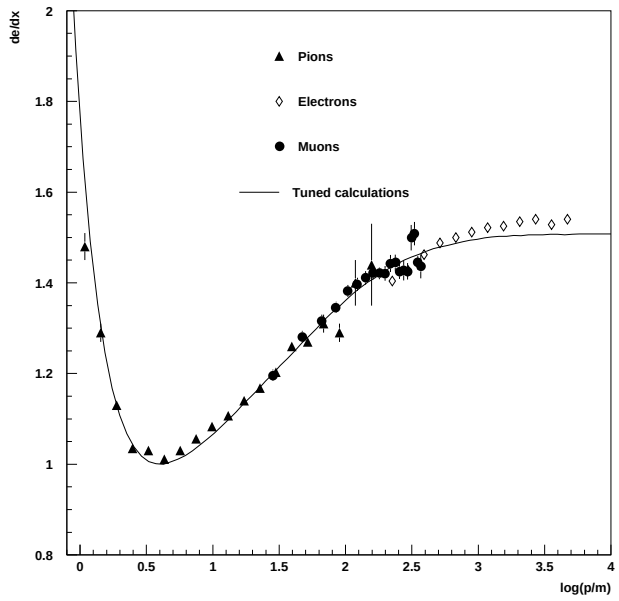

Figure 5: Truncated mean (80% lowest amplitudes kept) vs. $\beta\gamma$ (p/m). The filled circles are $\mu^{\pm}$ from τ decays, the filled pyramids are $\pi^{\pm}$ from K_s^0 decays and the diamonds are $e^{\pm}$ from photon conversions.

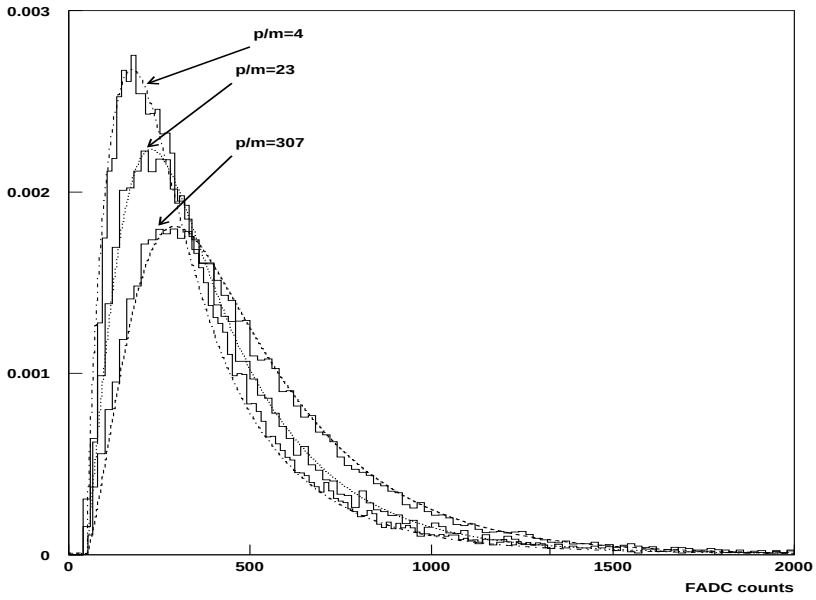

Figure 6: Calculated Landau distributions with a constant offset of 50 energy units vs. real data. A $n = 4$ approximation was used. The solid lines show the data for $p/m = 4$, 23 and 307 respectively where the latter was used for the tuning. The measured distribution for $p/m = 4$ was obtained with $\langle dE/dx \rangle$ tagging of minimum ionizing pions. One thus must take into account that it is biased to the $\langle dE/dx \rangle$ cuts used in the tagging.

7 Conclusions

We have in detail described a new method to obtain an accurate prediction of the ionization energy loss in proportional chamber detectors. The method relies on the assumption that all detector specific properties can be contained in a single effective dielectric function, which may be obtained from a well measured Landau distribution for a give particle velocity. The energy loss calculations are thus tuned to the detector and no further information like tabulation of the photoionization cross section or simulation of detector smearing should be needed.

A reasonable robust mathematical procedure to extract the effective dielectric function from the measured Landau distribution has been described and applied to data from the *Time Projection Chamber* in the DELPHI experiment at CERN. The results from this test show an excellent agreement between the data and the tuned dE/dx calculations in particular if the low energy offset in the measured distribution is taken into account.

Acknowledgements

I wish to thank my colleagues in the DELPHI TPC group for providing me with data. In particular Drs. Laurent Chevalier, Ahmimed Ouraou and Pierre Antilogus for fruitful discussions and helping me with the extraction of the TPC data. Dr. Mogens Dam deserves a special thank for his work to tag tau events and identifying the decay products with other means than dE/dx.

I am greatly indebted to Prof. Göran Jarlskog and Dr. Bengt Lörstad for reading and criticizing the paper.

The work presented in this paper has been going on for more than two years with financial support from three different institutes to whom I wish express my gratitude: LAL, Orsay/France, the Swedish Natural Science Research Council and CERN, Geneva/Switzerland.

References

[1] L.Landau, J.Phys. USSR 8 (1944) 201

[2] E.Lindelöf, Le Calcul des Résidus et ses Applications a la Théorie des Fonctions, Chelsea Publishing Company, N.Y., (1947)

[3] F.Lapique and F.Piuz, Nucl. Instr. Methods, 175 (1980) 297;

[4] H.H.Umstaetter, Documentation on The CERN Program Library entry C204.

[5] C.Brand et al., IEEE Trans. Nucl. Sci. NS-36 (1989) 122;
C.Brand et al., Nucl. Instr. Methods A283 (1989) 567;

[6] O.Bärring: Nucl. Instr. Methods A284 (1989) 459